

*Full Paper*

## **Biomedical Application of a Novel Nanostructured-based Electrochemical Platform for Therapeutic Monitoring of an Antiepileptic Drug; Gabapentin**

**Atieh Zabihollahpoor,<sup>1</sup> Mostafa Rahimnejad,<sup>1,\*</sup> Ghasem Najafpour-Darzi,<sup>2</sup>  
and Ali Akbar Moghadamnia<sup>3</sup>**

<sup>1</sup>*Biofuel and Renewable Energy Research Center, Department of Chemical Engineering, BabolNoshirvani University of Technology, Babol, Iran*

<sup>2</sup>*Biotechnology Research Laboratory, Faculty of Chemical Engineering, BabolNoshirvani University of Technology, Babol, Iran*

<sup>3</sup>*Faculty of Pharmacology, Babol University of Medical Sciences, Babol, Iran*

\*Corresponding author, Tel.: +981132313516; Fax: +9811132334204

E-mail address: [Rahimnejad@nit.ac.ir](mailto:Rahimnejad@nit.ac.ir)

*Received: 20 March 2020 / Received in revised form: 20 April 2020 /*

*Accepted: 17 April 2020 / Published online: 30 April 2020*

---

**Abstract-** Herein, gold nanoparticle had been successfully synthesized through a simple, inexpensive and clean electrochemical technique. Gold nanoparticles were directly deposited on the electrode surface using an electrochemical strategy. Then, the electrochemical deposition parameters (such as applied potential and deposition time) were optimized. 1.1 V and 250 s were applied as the optimal electrodeposition potential and time in the rest of the investigations. The fabricated electrode was morphologically characterized by field emission scanning electron microscopy and energy-dispersive X-ray spectroscopy methods. Under the optimized condition, the proposed sensor demonstrated the lowest detection limit (7.04 nM) in the linear range of 0.01–1  $\mu$ M obtained by differential pulse voltammetry. The electrochemical properties of fabricated modified electrode were investigated by a different techniques such as cyclic voltammetry, linear sweep voltammetry, differential pulse voltammetry, and electrochemical impedance spectroscopy. The constructed electrode also showed a negligible response from common interferences and the fabricated sensor was applied for Gabapentin analysis in pharmaceutical samples.

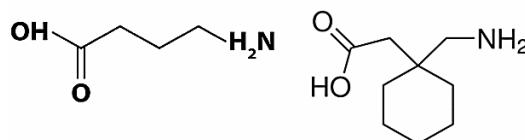
**Keywords-** Gold nanoparticles; Graphene nanoplatelets; Electrodeposition; Gabapentin; Electrochemical sensor; Blood plasma

---

## 1. INTRODUCTION

$\gamma$ -aminobutyric acid (GABA) as one of the important inhibitory neurotransmitters in human brain made from glutamate. It plays a vital role in blocking the nervous pulses [1]. Low activity of GABA could result in uncontrolled electrical impulses in the brain cells leading to several brain disorders (i.e. partial seizures).

Gabapentin (GP) with the chemical structure of [1-(amino methyl) cyclohexane acetic acid] is developed as a GABA-mimetic compound with an incorporated lipophilic cyclohexane ring (Scheme 1) [2]. It alters GABA transmission in the central nervous system and facilitates crossing the blood–brain barrier [3]. It also increases the extracellular GABA concentration produced by glutamic acid decarboxylase and decreases GABA degradation into other amino acids through GABA-transaminase inhibition [2,3].



**Scheme 1.** Chemical structure of GABA (left) and Gabapentin (right)

In this regard, development of a suitable (sensitive and reliable) method for monitoring of serum concentration of anti-epileptic drug (AED) is of vital importance. So far, various analytical techniques including gas chromatography (GC), capillary electrophoresis (CE) and high performance liquid chromatography (HPLC) have been applied for GP detection [4,5]. But the use of electrochemical method has recently attracted more attention as it is an facile, low cost, sensitive and fast technique [6].

Carbon paste electrodes (CPEs) have been widely used for electrochemical purposes due to their cost-effectiveness, ease of modification, good reproducibility, high sensitivity and renewability (the surface can be renewed by polishing) [7-9]. To improve the mentioned features, bulk or surface composition of CPE can be modified by incorporating a desired material. To date, several nanostructured materials, such as multiwall carbon nanotubes [5], copper sulfide nanostructures [10], silver nanoparticles [11] and nickel nanotubes [12] have been employed for selective and sensitive GP detection. However, there is no report on application of graphene nanoplatelets (GRNP) and Gold nanoparticle (GNP) in electrochemical sensing of GP.

GRNP is a single flat sheet of graphite. Owing to its wonderful electronic transport properties, suitable chemical stability, high surface area to volume ratio, great mechanical strength and high electrocatalytic activities [13-16], it has been regarded as an attractive material in experiences related to electrochemistry such as electrochemical sensors. Further modification of CPE surface is achievable by nano-sized gold structures. Due to its unique properties including large surface area, low toxicity, good conductivity, useful

electrocatalytic characteristics, and excellent biocompatibility, GNP has attracted a considerable deal of attention for modification of various electrodes [7,17-20]. GNP can also improve the stability and sensitivity of graphene-based electrodes by the synergistic effects [21,22]. Several approaches including self-assembly and seed-mediated growth methods have been employed to obtain gold nanoparticles [18,19,23]. In this study, GNPs were fabricated through a simple, rapid and clean electrochemical technique (electrodeposition). The size and morphology of GNPs deposited on CPE can be controlled by varying the deposition time, gold salt concentration, pH and deposition potential [23].

Herein, both GNP and GRNP have been studied for fabrication of an electrochemical sensor. The prepared electrode was evaluated for use in electrochemical analysis of GP using different voltammetric techniques.

## 2. EXPERIMENTAL SECTION

### 2.1. Chemicals and solutions

Pure GP powder was supplied by Actoverco (Tehran, Iran). Graphene nanoplatelets (99.5+%, 2-18 nm with 32 layer) was purchased from US Research Nanomaterials, Inc. (Houston, USA). Gabax tablets (sobhandarou CO., Tehran, Iran) labeled to contain 100 mg of gabapentin were provided from local markets. Analytical grade  $\text{HAuCl}_4 \cdot 3\text{H}_2\text{O}$  was purchased from Merck. 100mM stock solution of GP was prepared with distilled water. NaOH-based Buffer solutions (with different pH) were prepared with analytical grade reagents according to Table 1. All other chemicals used in this study were of analytical grade and prepared by distilled water.

**Table 1.** Different supporting electrolytes

pH	Composition
8	$\text{KH}_2\text{PO}_4 + \text{NaOH}$
10	$\text{NaHCO}_3 + \text{NaOH}$
11	$\text{NaHCO}_3 + \text{NaOH}$
12	$\text{KCl} + \text{NaOH}$
13	$\text{KCl} + \text{NaOH}$

### 2.2. Apparatus

Potentiostat/Galvanostat IVIUM (Vertex, Netherlands) performed the voltammetric measurements of the developed electrochemical sensors. A usual three-electrode system comprising of a CPE as the working electrode (modified as described); an Ag/AgCl electrode in 3 M KCl as the reference electrode and a Pt electrode as an auxiliary one were used for all

the experiments. For pH measurements, the Mettler-Toledo pH-meter (model FE20/EL20) was applied in combination with a glass electrode.

Field emission scanning electron microscopy (FE-SEM) photographs were recorded using FEI Nova nanoSEM450 microscope was used for characterizing the CPE surface, morphology of GNPs and GRNP. GNPs were also characterized by an energy-dispersive X-ray spectroscopy (EDX) analysis (Bruker X flash61 10).

### **2.3. Fabrication of GRNP modified CPE**

The bare CPE was fabricated by manual mixing of a small amount of graphite powder with paraffin oil (70:30 percentage w/w). GRNP/CPE was also fabricated by manual mixing of an adequate amount of GRNP with graphite powder and paraffin oil (60:10:30 percentage w/w). After homogenization in a mortar and pestle, the paste was filed at the bottom end of a glass tube. A copper wire was fitted into the opposite end of the glass tube to enhance the electrical contact. Prior to each measurement, the surface of the fabricated electrode was mechanically polished with a paper sheet followed by cleaning with distilled water.

### **2.4. Electrochemical synthesis of GNP**

To construct GNP-modified CPE and GRNP/CPE, the unmodified electrode surface was first polished. Then, a potentiostatic technique [18,24] was used in a 0.5 mM solution of tetrachloroauric acid (prepared in distilled water) under stirring conditions. Deposition potential and deposition time were varied to obtain the optimum parameters.

### **2.5. Real sample preparation**

The GNP/GRNP-modified electrodes were evaluated for GP determination in two different matrix samples including commercial capsules and healthy plasma samples. To analyze the GP capsules, 10 capsules were weighted and finely ground in a mortar to break any aggregated material. Then the required amount of powder equivalent to a 10 mM stock solution GP was dissolve in distilled water and filtrated after sonication. Suitable aliquots of the filtered stock solution were further dilute in the range of calibration plot. The calibration plot obtained under the optimized condition was used for real concentration calculation. 0.2 ml plasma sample of a healthy volunteer was diluted with 40 ml buffer solution and spiked with known amount of standard drug sample. The calibration plot obtained under the optimized condition was used for real concentration calculation.

## **3. RESULTS AND DISCUSSION**

### **3.1. Physical Characterization of different prepared electrodes**

The surface morphology and structure of the sample electrodes were elucidated by FE-SEM. Separated layers of graphite flakes particles can be observed in the FE-SEM micrographs of bare CPE (Fig. 1a). Uniform and dispersed distributions of two-dimensional sheet of graphene nanoplatelets in CPE structure are depicted in Fig.1b. The white color in Fig1c indicated the formation of the metallic gold nanoparticles on electrode surface through electrodeposition technique. The GNPs in the unmodified and the GRNP-modified CPE were also mapped in FE-SEM images (insets of Fig. 2). These results were also confirmed from energy-dispersive X-ray spectroscopy (EDX) shown in Fig. 2. Clearly, the CPE and GRNP/CPE contained enough GNPs (2.28 and 5.62 wt. percentage respectively) for electrocatalysis. The average size of nanoparticles was found in the range of 200-500 nm.

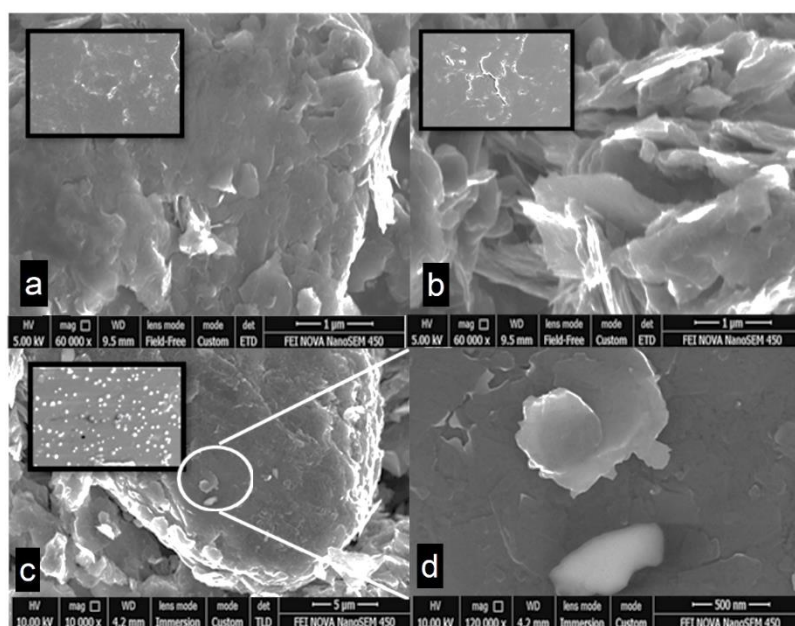


**Fig. 1.** SEM images of carbon paste (a) with graphene nanoplatelets (b) GNP and graphene nanoplatelets (c) and SEM image of GNP was magnified (d). The insets show the surface morphology of prepared electrodes

### 3.2. Optimization of electrodeposition method

As mentioned before, the GNPs were prepared by electrodeposition method. Therefore, several parameters can influence the morphology and surface area of the deposited GNP. To optimize the electrodeposition technique and hence improve the electron transfer efficiency between GP and surface of the modified electrode, the electrochemical results at the presence of GP were investigated by altering (a) deposition potential and (b) deposition time. Linear scanning voltammograms (LSV) were applied to address the electrochemical characterization of GNP-modified electrodes.

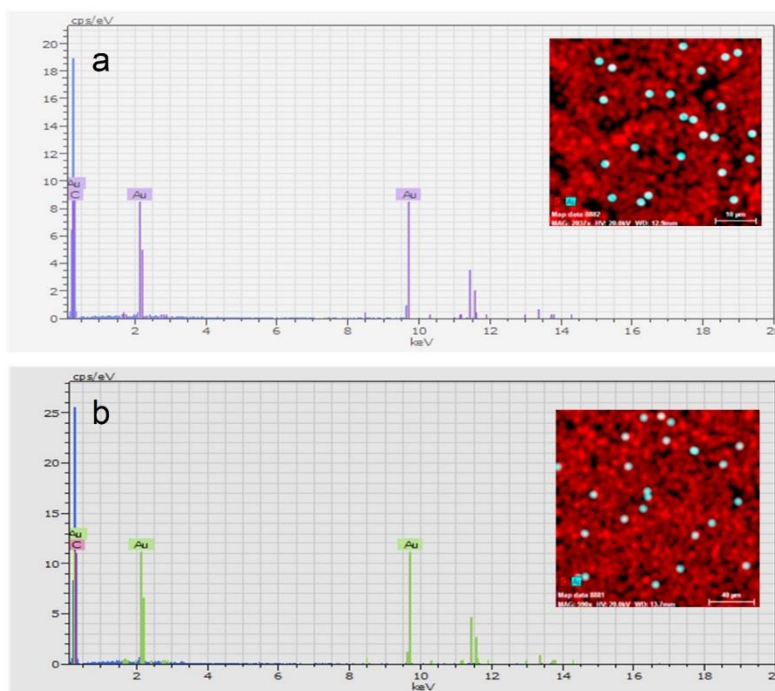


**Fig. 2.** EDX spectra of GNP modified CPE (a) and GNP/GRNP modified CPE (b) The insets show the SEM image of mapped GNP

### 3.2.1. Applied potential

One of the important factors to improve the electron transfer efficiency is the applied potential in electrodeposition technique. It was optimized by varying the reduction potential between  $-0.5$  V to  $-1.3$  V relative to Ag/AgCl. The potential was swept from zero to  $0.8$  V. Fig.3 shows the LSV diagrams of GNP/GRNP/CP electrode in the buffer solution containing  $10$  mM gabapentin. As can be seen, an oxidation peak appeared at approximately  $0.65$  V. The oxidation peak current increased with enhancement of the applied potential and remained constant beyond  $-1.1$  V. These observations can be justified as follows: the deposition potential has a significant impact on the morphology of GNPs, which can increase the active sites for electro-oxidation of gabapentin. Further increase of the potential beyond  $-1.1$  V did not enhance the electrochemical response of GNP/GRNP/CPE towards gabapentin oxidation. Therefore,  $-1.1$  V was applied as the optimal electrodeposition potential in the rest of investigations.

### 3.2.2. Deposition time

Electrodeposition time is the other significant factor with high impacts on the morphology of GNPs. Fig.4 shows the LSV diagrams of GNP/GRNP/CPE constructed by varying the electrodeposition time between  $10$  to  $600$  s. Increase of electrodeposition time enhanced the number of GNPs deposited on the electrode surface and consequently the effective surface

area for gabapentin oxidation which is consistent with the previous findings [18]. In order to shorten the experiments time, 250 s was applied as the optimum deposition time.

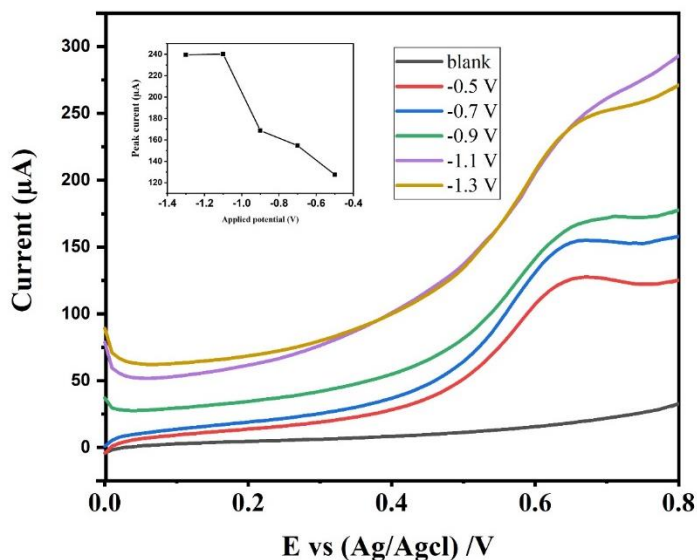


**Fig. 3.** Electrodeposition potential dependent of LSV diagrams at GNP/GRNP/CPE in NaOH+KCl buffer solution containing 10 mM of gabapentin and at scan rate of 100 mv/s. The inset demonstrates peak current vs. deposition potential

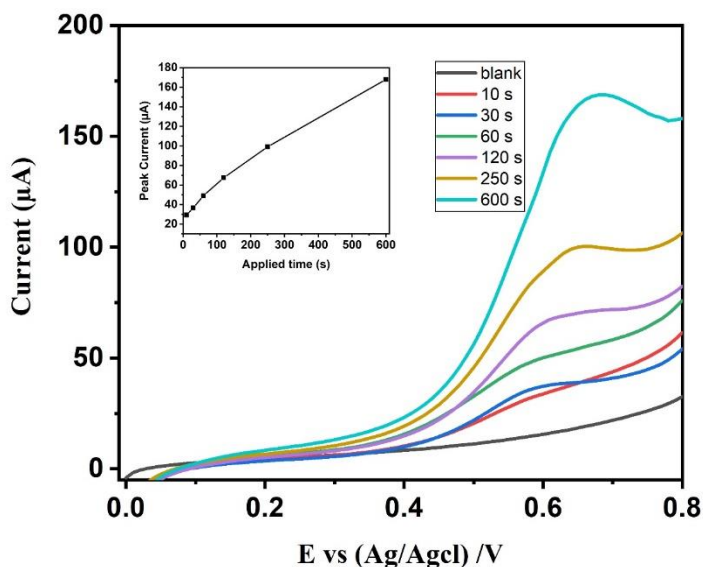


**Fig. 4.** Electrodeposition time dependent of LSV diagrams at GNP/GRNP/CPE in NaOH+KCl buffer solution containing 10 mM of gabapentin and at scan rate of 100 mv/s. The inset demonstrates peak current vs. time

### 3.3. Electrochemical properties of different modified CPEs

Electrochemical properties of the electrodes was investigated in 5 mM  $[\text{Fe}(\text{CN})_6]^{3-/4-}$  solution prepared by 1mM potassium chloride solution at the scan rate of 100 mV/s. Cyclic voltammetry (CV) and electrochemical impedance spectroscopy (EIS) are often used for electrochemical characterization of novel electrodes.

The CV diagrams of the pristine and modified CPE are shown in Fig.5. As is clear, the  $[\text{Fe}(\text{CN})_6]^{3-/4-}$  oxidation peak current at GRNP/CPE and GNP/CPE increased and was more reversible in comparison with the pristine CPE; which could be due to the good conductivity and catalytic properties of GRNP and GNPs. On the other hand, the presence of GRNP in the structure of GNP-modified CPE had no significant effect on its reversibility and increase of the currents of  $[\text{Fe}(\text{CN})_6]^{3-/4-}$  redox couple peak. As for the reversible operation of various modified CPE (According to  $I_p/I_{pc}$  ratio), Randles-Sevcik equation [25,26] was applied to calculate the electroactive area of these modified electrodes:

$$i_p = 2.69 \times 10^5 n^{3/2} D_0^{1/2} \nu^{1/2} C_0 A \quad (1)$$

where  $i_p$  is the peak current of the redox couple,  $n$  denotes the number of the transferred electrons ( $n=1$  for  $[\text{Fe}(\text{CN})_6]^{3-/4-}$  redox couple);  $D_0$  represents the diffusion coefficient ( $D_0 = 6.3 \times 10^{-6} \text{ cm}^2 \text{ s}^{-1}$  for  $[\text{Fe}(\text{CN})_6]^{3-/4-}$  redox couple in  $0.1 \text{ mol L}^{-1}$  KCl solution at  $25^\circ\text{C}$ ) [27];  $\nu$  is the scan rate (in V/s),  $C_0$  stands for the concentration (in  $\text{mol/cm}^3$ ) and  $A$  shows the electroactive surface area (in  $\text{cm}^2$ ). The calculated values of electroactive surface area are 0.20, 0.23, 0.337 and  $0.339 \text{ cm}^2$  for CPE, GRNP/CPE, GNP/CPE and GNP/GRNP/CPE respectively. Unlike the GRNP, GNPs significantly increased the electroactive surface area of the CPE.

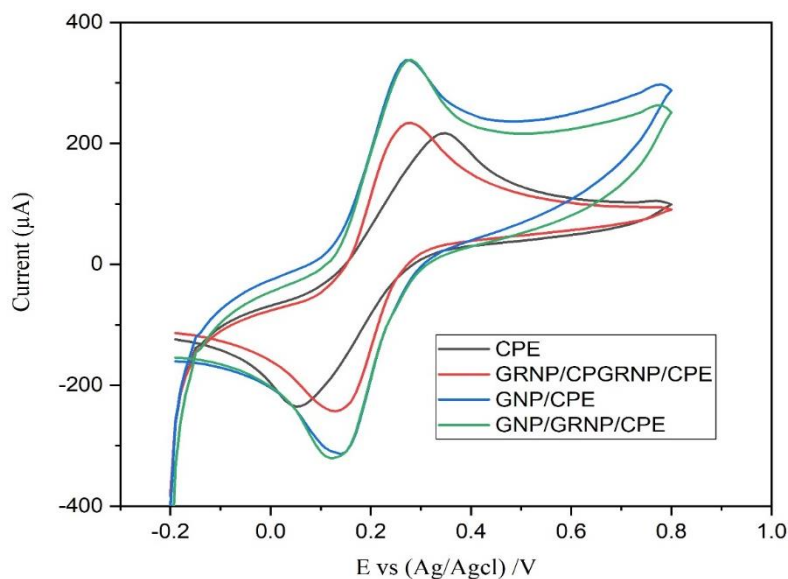


**Fig. 5.** CV diagrams of different modified electrodes in 5 mM  $[\text{Fe}(\text{CN})_6]^{3-/4-}$  solution prepared by 1mM potassium chloride solution at a scan rate of 100 mV/s

Charge transfer resistance of different modified electrodes was also investigated by EIS analysis. Fig.6 shows the Nyquist plots of pristine and modified CPE. All the plots are composed of a semicircular and a linear part corresponding to electron transfer and diffusion limited processes, respectively. Randles equivalent circuit (inset in Fig.6) can be used to model the detailed information in which  $R_s$ ,  $Z_w$ ,  $R_{ct}$  and  $C_{dl}$  are solution resistance ( $\Omega$ ), Warburg impedance, charge-transfer resistance ( $\Omega$ ) and interfacial capacitance, respectively. According to the calculated  $R_{ct}$  value, GNP and GRNP-modified electrodes exhibited the lowest charge-transfer resistance due to their high surface area and good conductivity. However, GRNP had lower effect to decrease the resistance of CPE probably due to its poor conductivity compared to GNP.

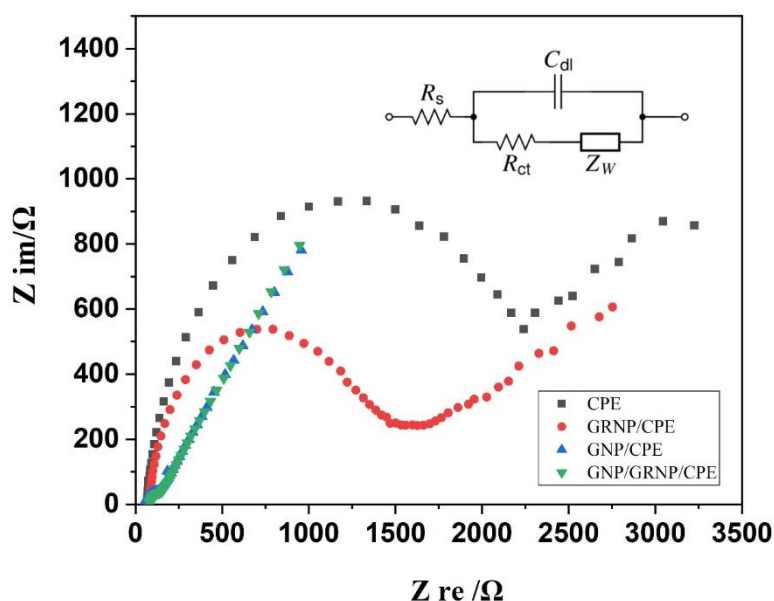


**Fig. 6.** EIS results of unmodified and modified electrodes in 5 mM  $[\text{Fe}(\text{CN})_6]^{3-/4-}$  solution prepared by 1mM potassium chloride obtained from impedance measurements; Inset: Randles equivalent circuit

### 3.4. Electrochemical oxidation of GP at GR/GNP/CPE

Electrochemical behavior of various modified CPEs was studied by CV technique in an electrolyte containing 10 mM solution of gabapentin (Fig. 7). While no redox peak was observed on the pristine CPE, a broad and tiny oxidation peak of gabapentin was observed on GRNP/CPE, which indicated the poor electrochemical activity of GRNP for gabapentin oxidation. On the other hand, the anodic peak of GNP/CPE significantly increased due to the enhanced electrochemical activity of GNPs. According to the comparisons, the signal of GNP/GRNP/CPE for gabapentin oxidation was obviously higher than that of GNP/CPE, reflecting the synergistic effect of GRNP and GNP for gabapentin oxidation. The presence of gabapentin resulted in shift of the oxidation peak of GNP/GRNP/CPE to positive potentials.

Moreover,  $I_{pa}/I_{pc}$  of gabapentin redox couple on GNP/GRNP/CPE was four, suggesting the irreversible behavior of gabapentin on the electrode surface. For an irreversible electrochemical process  $n$  can be obtained according to Eq. (2) [8,28]:

$$\Delta E_{pa} = E_{pa} - E_{pa/2} = \frac{47.7}{\alpha} mV \text{ (at 298k)} \quad (2)$$

where  $E_{pa/2}$  is the potential at the half peak current value and  $\alpha$  represents the electron transfer coefficient. In this investigation,  $\alpha$  was calculated as 0.366.

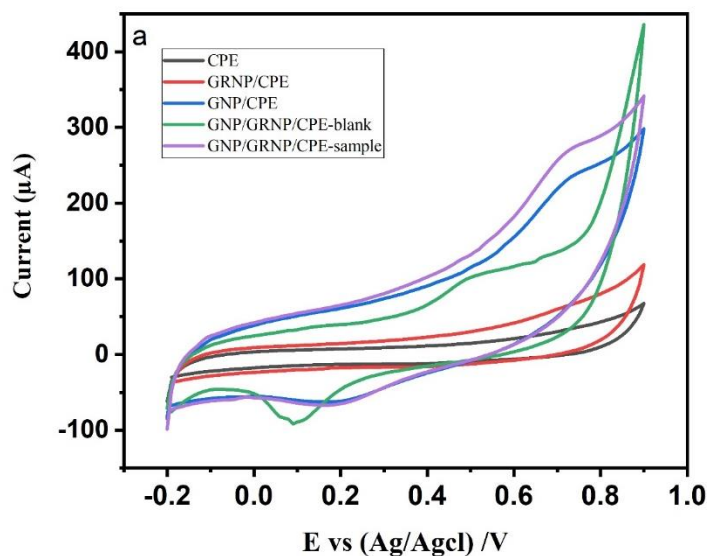


**Fig. 7.** CVs of bare and modified CPEs in in NaOH+KCl buffer solution containing 10 mM of gabapentin and at scan rate of 100mv/s and blank CV diagram of GNP/GRNP/CPE

### 3.5. The pH effect on electrochemical response of GP

The pH of electrolyte solution can affect the current of oxidation peak in different voltammetry techniques; it can also alter the mechanism of electrochemical oxidation. The CV response of GNP/GRNP/CPE to gabapentin was tested in pH range of 8.0-13 as shown in Fig.8. At  $pH < 8$ , the gabapentin oxidation peak disappeared as was reported before [5]. Maximum oxidation peak current of gabapentin was observed at  $pH=12$  (Fig. 8-inset). By increase of pH, the oxidation peak potential also shifted to less positive potentials due to faster and easier removal of electron from the gabapentin (amine group) in alkaline solution [29] (see Fig. 8-inset). The pH-dependence of the oxidation peak ( $E_p$ ) showed a linear relation with a regression equation of  $E_p \text{ (V)} = -0.0791 \text{ pH} + 1.5538$  ( $r^2=0.9903$ ) (Fig. 8-inset).

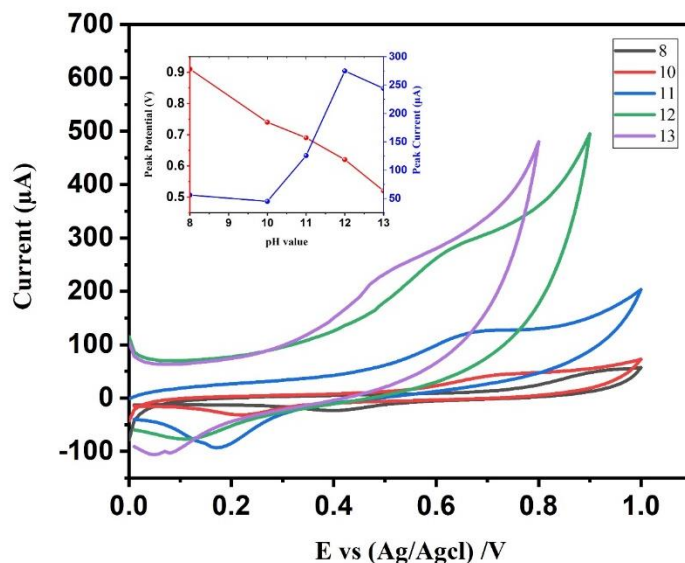


**Fig. 8.** The pH effects on CV diagrams of fabricated electrochemical sensor for gabapentin detection in buffer solution containing 10 mM of gabapentin and at scan rate of 100 mv/s, (inset) the potential and Current of oxidation peak vs. pH

### 3.6. Scan rate effect on electrochemical response of GP

The influence of scan rate on the electrochemical oxidation response of GNP/GRNP/CPE to gabapentin was also studied. Fig.9a represents the corresponding CV diagrams of GNP/GRNP/CPE at different scan rates (5-200 mV/s) in 10 mM gabapentin solution. The anodic peak current of gabapentin on GNP/GRNP/CPE linearly varied with  $\sqrt{\nu}$  which means that the oxidation reaction is diffusion-controlled (Fig. 9c). In addition, a positive shift in the anodic peak potential was observed by increasing the scan rate. Equation.3 [29-31] was used to explain the dependency of peak potential vs.  $\ln \nu$  (Depicted in Fig. 9b):

$$E_{pa} = E^{\circ} - \left( \frac{RT}{(1-\alpha)nF} \right) \ln \left( \frac{RTk^0}{(1-\alpha)nF} \right) + \left( \frac{RT}{(1-\alpha)nF} \right) \ln \nu \quad (3)$$

where,  $k^0$  is the standard rate constant for heterogeneous reaction and  $E^{\circ}$  shows the formal redox potential. According to linear regression equation, the slope is 0.059 and by taking  $R = 8.314 \text{ J K}^{-1} \text{ mol}^{-1}$ ,  $F = 96,480 \text{ C}$  and  $T = 298 \text{ K}$ ,  $(1-\alpha)n$  and  $n$  were calculated as  $\sim 1$ , respectively.  $E^{\circ}$  and  $k^0$  were calculated by extrapolating  $E_p - \nu$  curve and considering the linear regression equation. The calculated values of  $E^{\circ}$  and  $k^0$  are 0.572 V and  $953.64 \text{ s}^{-1}$ , respectively.

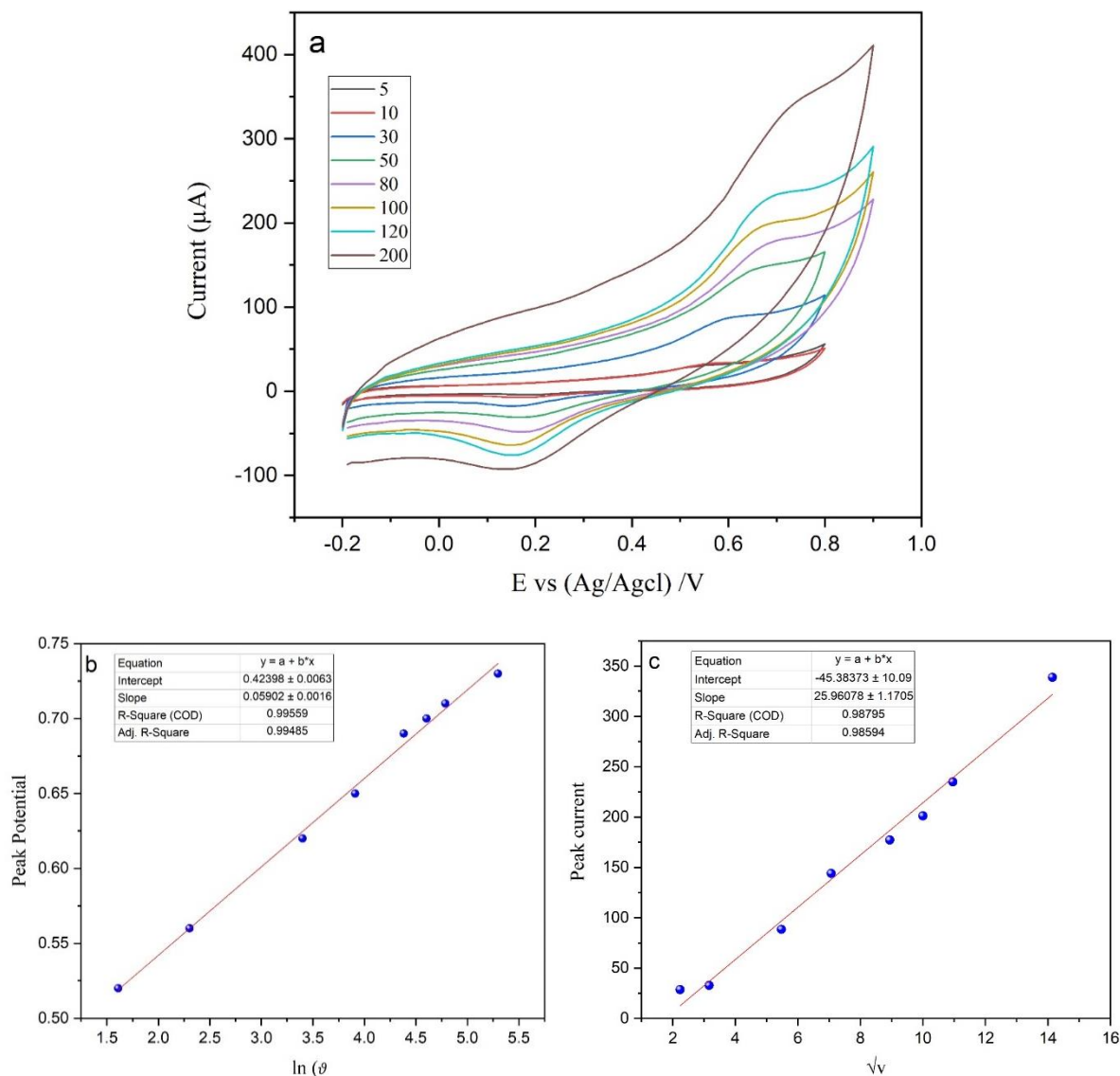


**Fig. 9. (a):** CVs of GNP/GRNP/CPE in NaOH+KCl buffer solution containing 10 mM of gabapentin and at different scan rates: (5, 10, 30, 50, 80, 100, 120 and 200mV/s), **(b):** The linear dependence of anodic peak potential vs.  $\ln(v)$  and **(c)** The linear dependence of  $I_{pa}$  vs.  $\sqrt{v}$

### 3.7. Electrochemical determination of GP using DPV

The DPV technique was applied to determine the linear oxidation range, limit of detection (LOD) and quantification (LOQ) of gabapentin on GNP/GRNP/CPE. The peak potential shift in the DPV tests in compared with the CV test is very low (Fig. 10a). It is due to the very low concentration of the drug in the buffer solution in DPV tests. As can be seen in the inset of Fig. 10a, at higher concentration of gabapentin the potential peak shifts to values that are more positive, the same as CV tests.

As indicated in Fig.10a, the linear range of electrode is 0.01-1  $\mu\text{M}$  and the current of oxidation peak was linearly increased with concentration enhancement. According to linear

calibration curves (Fig.10b) and the linear equation ( $I_p (\mu\text{A}) = 5.48C (\text{GP}) + 29.73$  ( $r^2 = 0.98$ )), LOD was found to be 7.04 nM:

$$LOD = \frac{3\sigma}{m} \quad (4)$$

where  $\sigma$  is the standard deviation obtained for blank signals and  $m$  shows the slope of calibration [29, 32]. The functionality of the fabricated electrode was compared with different modified electrodes as listed in Table 2.

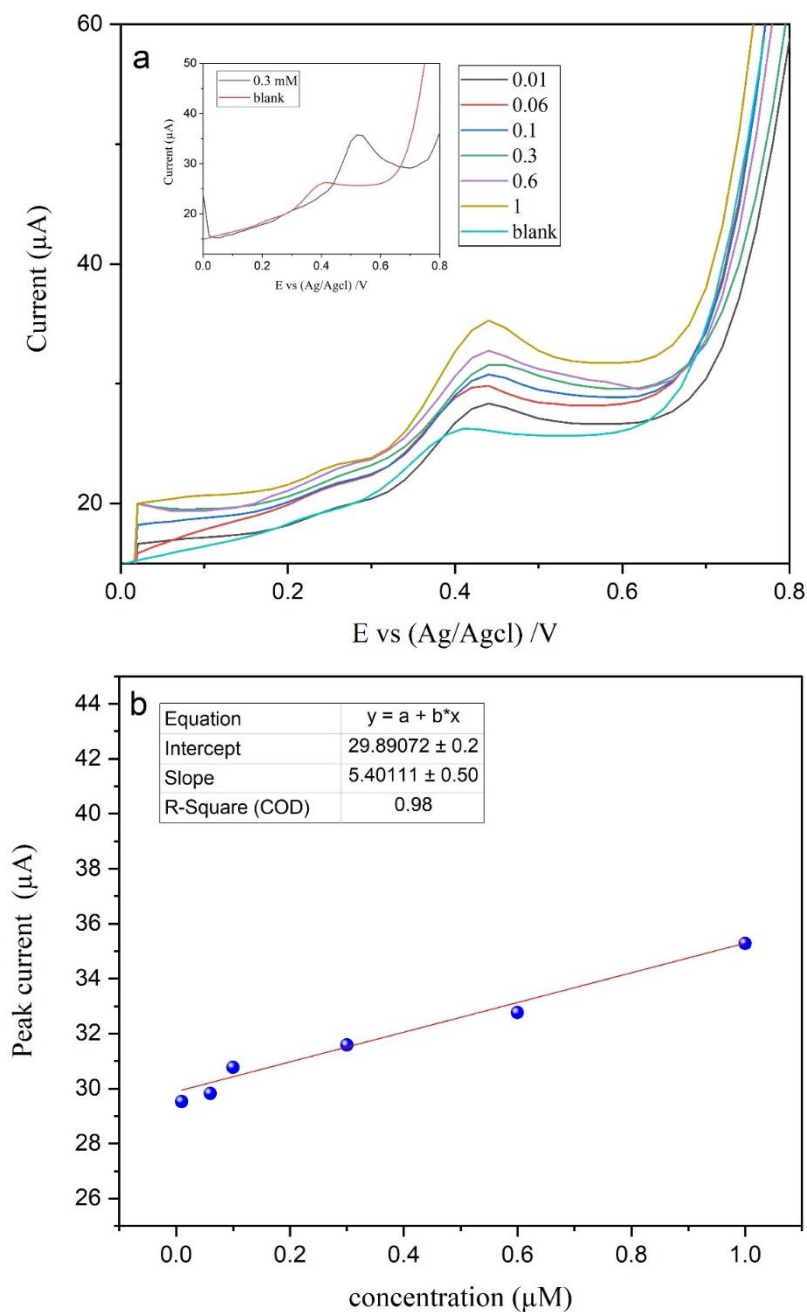


**Fig. 10. (a):** DPV plots of GNP/GRNP/CPE in buffer solution at different gabapentin concentration. The inset: The positive shifting of peak potential at high gabapentin concentration, **(b):** The linear dependence of  $I_{pa}$  vs. GP concentration ( $n=3$ )

**Table 2.** A comparison between GNP/GR/CPE and other modified electrodes for gabapentin determination

Electrode	Modifier	Method	Linear range ( $\mu\text{M}$ )	LOD ( $\mu\text{M}$ )	Ref.
Bare gold	-	DPV	0.3–15	0.13	[29]
CPE	Nickel oxide nano tubes	Amp	2.4–50	0.3	[12]
Carbon Ceramic	CNT/Ni-Catechol	LSV	1.23-63.23	0.5	[5]
Glassy carbon	Gold nanoparticle	DPV	10-1000	3.25	[33]
CPE	GRNP/GNP	DPV	0.01-1	0.00704	This work

CNT: Carbon nanotubes, Amp: Amperometric.

### 3.8. Selectivity of sensing platform

In order to investigate the GNP/GRNP/CPE selectivity, cyclic voltammograms experiments were performed on 0.1 mM gabapentin, 10 mM of some co-formulated components in real samples and Valproic acid (usually used in combination with Gabapentin). The results (Table.3) showed no noticeable effect on Gabapentin peak current at the surface of GNP/GRNP/CPE.

### 3.9. GP detection on real sample

The applicability of GNP/GRNP/CPE was investigated by analyzing GP in commercial capsules and plasma through standard addition method. The obtained quantitative recoveries value (Table 4) confirmed that the proposed sensor could be used for quantitative Gabapentin determination.

**Table 3.** Various interferences examined with the constructed electrochemical sensor (n=3)

Various interference	Tolerance limit	Current ratio	RSD%
Valproic acid	100	1.01	4.5
K <sup>+</sup>	100	1.01	0.34
Cl <sup>-</sup>	100	1.00	0.59
Na <sup>+</sup>	100	0.9	7.28
Ca <sup>+</sup>	100	1.00	0.59
CO <sub>3</sub> <sup>2-</sup>	100	1.02	5.9
Urea	100	0.97	3.24
Starch	100	1.05	8.79
Citric acid	1	1.11	8.01
Oxalic acid	1	1.01	4.45
Uric acid	1	1.15	0.64

**Table 4.** Determination of Gabapentin in real sample (n=3)

Sample	Labeled (mg/capsule)	Founded ( $\mu\text{M}$ )	Recovery (%)	RSD%
Capsule	100	101	101%	5.9

Sample	Added ( $\mu\text{M}$ )	Founded ( $\mu\text{M}$ )	Recovery (%)	RSD%
Plasma	1	1.11	111%	5.87

#### 4. CONCLUSION

In summary, a gold nanoparticle and graphene nanoplatelets based CPE was fabricated to be used as a sensitive electrochemical sensor for Gabapentin analysis in biomedical samples. For this purpose, GRNP was mixed with carbon paste and GNP was electrochemically deposited on the paste surface. The GNP/GRNP/CPE showed an oxidation peak shift to more positive potentials with higher current values at the presence of Gabapentin. The LOD of the constructed sensor was  $0.00704 \mu\text{M}$  with linear concentration range of  $0.01\text{-}1 \mu\text{M}$ . Finally, The GNP/GRNP/CPE was applied for gabapentin detection in real samples which showed promising results.

#### Acknowledgement

This research was supported by the the Biofuel & Renewable Energy Research Center at BabolNoshirvani University of Technology (Grant number: BNUT/935150003/95).

#### Conflict of interest

On behalf of all authors, the corresponding author states that there is no conflict of interest.

#### REFERENCES

- [1] S. Zafar, M. E. Nguyen, R. Muthyala, I. Jabeen, and Y. Y. Sham, *Comput. Struct. Biotech. J.* 17 (2019) 61.
- [2] M. A. Rose, and P. Kam, *Anaesthesia* 57 (2002) 451.
- [3] F. Jalali, P. S. Dorraji, and H. Mahdiuni, *J. Lumin.* 148 (2014) 347.
- [4] M. El-Tohamy, S. Razeq, and A. Shalaby, *Int. J. Electrochem. Sci.* 7 (2012) 5374.
- [5] F. Jalali, Z. Hassanvand, and P. S. Dorraji, *J. Brazil. Chem. Soc.* 25 (2014) 1537.
- [6] Y. -R. Yuan, R. Yuan, Y. -Q. Chai, Y. Zhuo, and X. -M. Miao, *J. Electroanal. Chem.* 626 (2009) 6.

- [7] A. Afkhami, F. Soltani-Felehgari, and T. Madrakian, *Electrochim. Acta* 103 (2013) 125.
- [8] T. A. Saleh, K. M. AlAqad, and A. Rahim, *J. Mol. Liq.* 256 (2018) 39.
- [9] T. Alizadeh, and S. Amjadi, *Anal. Bioanal. Electrochem.* 12 (2020) 250.
- [10] G. Karim-Nezhad, and S. Pashazadeh, *Iranian Seminar of Analytical Chemistry, Ahvaz, Iran* 21 (2015).
- [11] A. Yari, F. Papi, and S. Farhadi, *Electroanalysis* 23 (2011) 2949.
- [12] H. Heli, F. Faramarzi, and N. Sattarahmady, *J. Solid State Electrochem.* 16 (2012) 45.
- [13] K. M. AlAqad, R. Suleiman, O. C. S. Al Hamouz, and T. A. Saleh, *J. Mol. Liq.* 252 (2018) 75.
- [14] Y. Dong, Y. Zhou, Y. Ding, X. Chu, and C. Wang, *Anal. Meth.* 6 (2014) 9367.
- [15] X. Chen, J. Liu, K. Qian, and J. Wang, *RSC Advances* 8 (2018) 10948.
- [16] P. Ekabutr, W. Klinkajon, P. Sangsanoh, O. Chailapakul, P. Niamlang, T. Khampieng, and P. Supaphol, *Anal. Meth.* 10 (2018) 874.
- [17] V. W. S. Hung, and K. Kerman, *Electrochem. Commun.* 13 (2011) 328.
- [18] H. Shu, L. Cao, G. Chang, H. He, Y. Zhang, and Y. He, *Electrochimica acta* 132 (2014) 524.
- [19] N. Elahi, M. Kamali, and M. H. Baghersad, *Talanta* 184 (2018) 537.
- [20] A. A. Habib, H. A. M. Hendawy, S. F. Hammad, L. I. Bebawy, and M. A. Girges, *Anal. Bioanal. Electrochem.* 12 (2020) 223.
- [21] I. Cesarino, R. P. Simões, F. C. Lavarda, and A. Batagin-Neto, *Electrochim. Acta* 192 (2016) 8.
- [22] H. Z. Pan, H. W. Yu, N. Wang, Z. Zhang, G. C. Wan, H. Liu, X. Guan, and D. Chang, *J. Biotechnol.* 214 (2015) 133.
- [23] L. Wang, W. Mao, D. Ni, J. Di, Y. Wu, and Y. Tu, *Electrochem. Commun.* 10 (2008) 673.
- [24] W. Ye, J. Yan, Q. Ye, and F. Zhou, *J. Phys. Chem. C* 114 (2010) 15617.
- [25] L. Li, T. Zhou, G. Sun, Z. Li, W. Yang, J. Jia, and G. Yang, *Electrochim. Acta* 152 (2015) 31.
- [26] M. M. Vinay, Y. A. Nayaka, K. V. Basavarajappa, P. Manjunatha, and H. Thimmappa, *Anal. Bioanal. Electrochem.* 12 (2020) 155.
- [27] I. M. Apetrei, and C. Apetrei, *International journal of nanomedicine* 11 (2016) 1859.
- [28] A. J. Bard, L. R. Faulkner, J. Leddy, and C. G. Zoski, *Electrochemical methods: fundamentals and applications*, wiley New York (1980).
- [29] R. N. Hegde, B. K. Swamy, N. P. Shetti, and S. T. Nandibewoor, *J. Electroanal. Chem.* 635 (2009) 51.
- [30] H. Ezoji, and M. Rahimnejad, *Int. J. Sci. Eng. Res.* 7 (2016) 242.
- [31] H. Ezoji, and M. Rahimnejad, *Sens. Actuat. B* 274 (2018) 370.
- [32] M. A. Prathap, R. Srivastava, and B. Satpati, *Electrochim. Acta* 114 (2013) 285.

- [33] A. Zabihollahpoor, M. Rahimnejad, G. Najafpour, and A. A. Moghadamnia, J. Electroanal. Chem. 12 (2019) 281.